Lasers in Manufacturing Conference 2015

Fabrication of graphene-chitosan electrodes films for sensing applications by laser-induced modification of the composite film

Romualdas Trusovas[a]*, Raiminda Celiešiūtė[b], Rasa Pauliukaite[b], Gediminas Račiukaitis[a]

[a] *Department of Laser Technologies, Center for Physical Sciences and Technology, Savanoriu Ave. 231, LT-02300 Vilnius, Lithuania*
[b] *Department of Nanoengineering, Center for Physical Sciences and Technology, Savanoriu Ave. 231, LT-02300 Vilnius, Lithuania*

Abstract

Graphene based electrodes have already shown an advantage in electro-catalytic activity and macroscopic scale conductivity. Formation of uniform graphene structure remains a significant challenge. Lasers have been already shown as useful tool for formation and modification of graphene structures.
In this research, we present our results on formation graphene-chitosan electrodes by a picosecond laser irradiation of the active film. Graphene was casted by a spin-coating from the weak acidic dispersion of the chitosan solution on the ITO electrode surface, and the laser treatment was applied for regular nanostructure formation.
Modified electrodes were investigated applying the cyclic voltammetry (CV) and electrochemical impedance spectroscopy (EIS). The same characterization was performed after the laser treatment of the samples. Experimental setup of laser treatment included picosecond laser (Atlantic, 10 ps, 100 kHz, Ekspla) working at the 1064 nm and 532 nm wavelength and the galvanometric scanner with a focusing objective (F=80 mm). Picosecond laser parameters and GO concentration were optimized according to the capacitance and the resistance changes, calculated from the EIS data of the laser-modified electrodes. The Raman spectroscopy showed that laser irradiation can cut out graphene sheets in the graphene-chitosan composites into smaller pieces inducing more edge defects. Moreover, laser irradiation with the average power higher than 150 mW, caused an increase in capacitance at the electrode surface due to the formation of nanocrystals of graphene.

Keywords: graphene; chitosan; picosecond laser; electrode;

* Corresponding author. Tel.: +370-672-49-107.
E-mail address: romualdas.trusovas@ftmc.lt

1. Introduction

Superior conducting properties, chemical purity and large surface area make graphene a promising candidate for sensors applications. Graphene is a two-dimensional material. Thus, all carbon atoms in the volume are exposed to the analyte of interest. It is a highly conductive material. A small number of crystal defects in a pristine graphene ensure a low level of noise caused by thermal switching (Choi et al., 2010).

In this research, results of laser-induced modification of the graphene-chitosan films, which intend to be used as a biosensor electrode, are presented. During the experiments, the laser irradiation power was varied, and the beam scanning speed was constant – 300 mm/s. The modified samples were investigated with SEM and Raman spectroscopy. For the electrochemical investigation of the modified composite films, methods of the cyclic voltammetry (CV) and electrochemical impedance spectroscopy (EIS) were applied.

Chitosan matrix was chosen to ensure even distribution of graphene flakes through the electrode surface. Previous attempts to cover the surface of the electrode with a uniform layer of graphene, using aqueous graphene suspensions failed due to agglomeration of graphene. Use of chitosan allowed to implement uniform distributions of graphene flakes and increased the mechanical stability of the electrode.

2. Experimental

2.1. Samples

Graphene flakes, obtained from Graphene Supermarket (USA), were additionally exfoliated and functionalized with hydroxy and carboxy groups. Then the aqueous solution of 0.5% chitosan was prepared. Functionalized graphene was added to the solution and sonicated for two hours untill a homogeneous dispersion was obtained. Suspensions of various concentrations (Table 1) were prepared according to these procedures. Suspensions were spin-coated on the indium-tin-oxide (ITO) square electrodes, then the electrodes were left to dry and later characterized applying Cyclic voltammetry and Electrochemical Impedance Spectroscopy. The thickness of the graphene-chitosan film was ~1 µm.

Table 1 Samples and their graphene suspensions concentrations.

Sample	G1	G2	G3	G4
Concentration	10 pg/ml	10 µg/ml	1 mg/ml	3 mg/ml

2.2. Laser treatment setup

Laser irradiation of the graphene chitosan composite films was performed with the picosecond laser (Atlantic, 10 ps, 100 kHz, 1064 nm, and 532 nm, Ekspla) (Fig. 1). The scanning speed was varied from 50 to 300 mm/s, and the applied mean laser power was ranged from 50 mW to 200 mW. Beam spot diameter at the focus was 20 µm. The graphene-chitosan composite was modified by applying hatch pattern, which means that lines with a certain distance (hatch) between them (20 µm) were scribed on the sample surface.

In order to achieve more uniform structuring, a different approach was chosen. In this approach, pulse overlapping was selected to be equal in both X and Y directions. In X direction, it was varied by means of changing the scanning speed and in Y – by changing the hatching period. A pitch parameter was introduced to reflect this type of overlapping. It stands for the distance between adjacent pulses in X/Y directions. The values of the used scanning speeds and hatch periods are shown in Table 2.

Seven values of pitch parameter were investigated (Table 2), and the laser power was varied from 10 mW

to 500 mW. Radiation of picosecond laser at two different wavelengths (1064 nm and 532 nm) was used in these experiments.

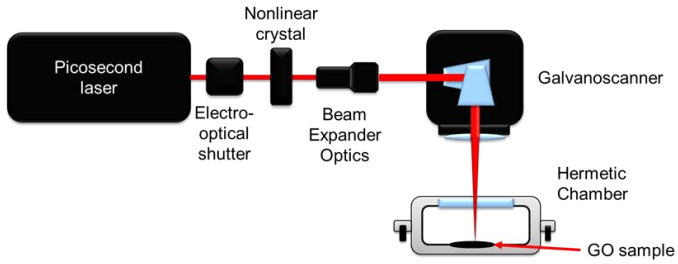

Fig. 1 Experimental setup for laser treatment of graphite oxide films.

Table 2 Pitch values and corresponding scanning speed and hatched period at the 100 kHz pulse repetition rate.

Pitch, μm	1	2	3	4	5	6	7
Scanning speed, mm/s	100	200	300	400	500	600	700
Hatch period, μm	1	2	3	4	5	6	7

Raman spectroscopy measurements of the graphene-chitosan composite films were performed with the Raman microscope inVia (Renishaw, UK) equipped with the thermoelectrically cooled CCD detector and using four different excitation wavelengths: 442 nm (0.8 mW) line from a He-Cd laser, 532 nm (0.6 mW) from a diode-pumped solid state laser, 633 nm (0.5 mW) from a He-Ne laser, and 785 nm (1.8 mW) from a diode laser. Raman spectra were taken using a 50x/0.75 NA objective lens. Integration time was 50 s. The wavenumber axis was calibrated according to the Si line at 520.7 cm^{-1}. Frequencies and intensities of the Raman bands were determined by fitting the experimental contour with the Gaussian-Lorentzian form components. Spectral analysis was performed by using GRAMS/A1 8.0 (Thermo Scientific, USA) software.

The scanning electron microscope JSM-6490 LV (JEOL) was used for investigation of surface morphology changes during the laser treatment. Samples without any additional preparation were used in the SEM microscopy.

Cyclic voltammetry and electrochemical impedance spectroscopy measurements were conducted with CompactStat potentiostat/galvanostat with the impedance module (Ivium Technologies, The Netherlands). The three-electrode system was used. Bare or graphene modified ITO was employed as a working electrode, Pt wire was as a counter electrode and Ag/AgCl (KCl sat.) electrode served as a reference. The same setup was used to perform EIS at a constantly applied potential, with the potential perturbation by 10 mV in the frequency range from 100 kHz to 0.1 Hz.

3. Results

3.1. Raman spectroscopy and morphology

Laser irradiation induced the reduction in the graphene-chitosan film thickness (

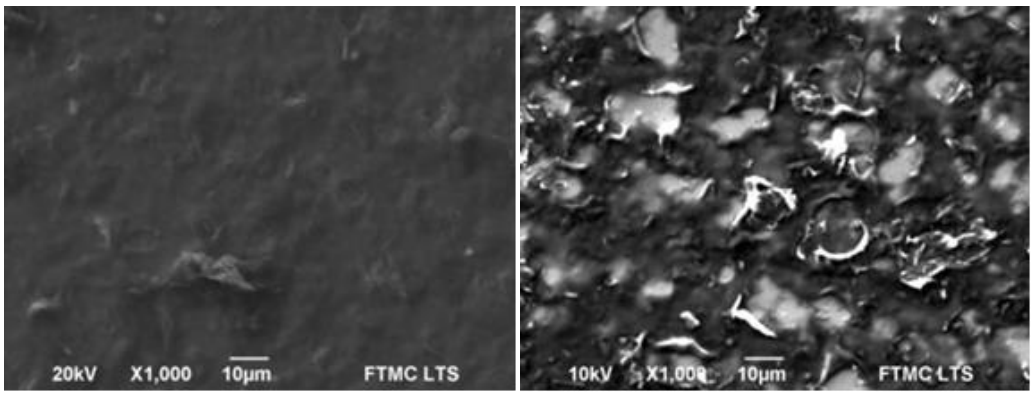

(a) (b)

). The thickness of the modified film strongly depended on the applied laser irradiation dose. Simultaneously, the surface morphology changes induced by the laser irradiation increased with the increasing irradiation dose. Chitosan was evaporated by the laser irradiation and graphene flakes were exposed with the rise of the picosecond laser irradiation dose (Fig. 3 b). Since more graphene edges were opened, the D-band was enhanced in Raman spectra after the laser treatment. In addition, according to the Raman spectra, more edge defects were observed after the laser treatment, which is in good agreement with the SEM morphology images.

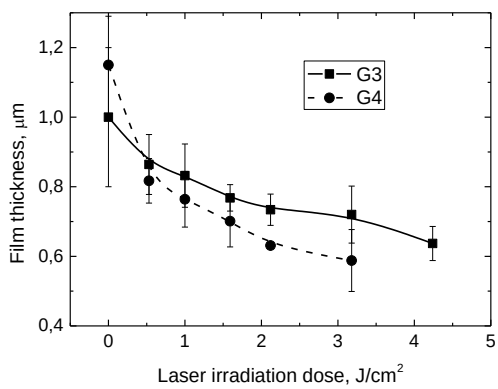

Fig. 2 Dependence of the graphene-chitosan film thickness on the laser irradiation dose.

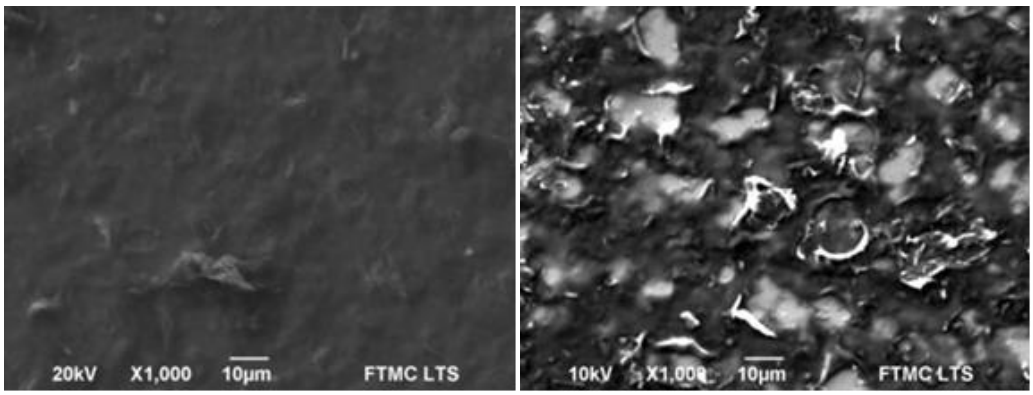

(a) (b)

Fig. 3 SEM images of untreated (s) and treated (b) with irradiation dose 3.34 J/ cm² G4 sample

Raman spectra revealed the development of broad D- and G-features using the high laser irradiation dose Fig. 4. The appearance of broad bands evidenced that the laser treatment induced formation of highly disordered carbon clusters. In the case of sample G4 (Fig. 4), at the low laser irradiation dose (1 J/cm^2), the shift of the G-peak to lower wavenumbers occurred. The lower wavenumber of the G-peak (1545 cm^{-1}) compared to untreated film (1581 cm^{-1}) was visible in the case of the treatment by the 2.12 J/cm^2 laser irradiation dose (Fig. 4). At all irradiation doses, the D- and G-peaks were present, and the I_D/I_G ratio was indicating the formation of the highly disordered nanocrystalline graphite (Fig. 4 b).

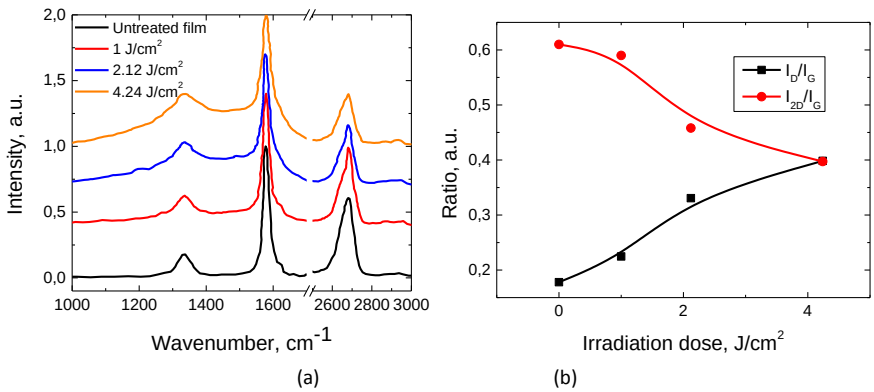

Fig. 4 Raman spectra (a) and dependence of the ID/IG and I2D/IG ratios in the G4 samples at different irradiation doses applied (b).

Dispersion analysis of the G-peak can be used to evaluate the degree of disorder in carbonous materials by means of multi-wavelength Raman spectroscopy (Ferrari et al., 2000) . The G-peak dispersion is a feature of the highly disordered carbon. This dispersion is proportional to the degree of disorder. The G-peak dispersion was observed in crystalline or nanocrystalline graphite (Ferrari et al., 2000, Wang et al., 1998) . The shift of the D-band towards lower wavenumbers was clearly visible with an increase in the excitation wavelength. No such shift was detectable for the G-band (Fig. 5). Quantitative analysis of the peak positions showed the D-peak dispersion of ~53 cm^{-1}/eV. The absence of the G-peak dispersion for the G3 and G4

samples indicated that the laser treatment with the 4.25 J/cm^2 irradiation dose formed the disordered nanocrystalline graphite, but not amorphous carbon (Celieš iūtė et al., 2014).

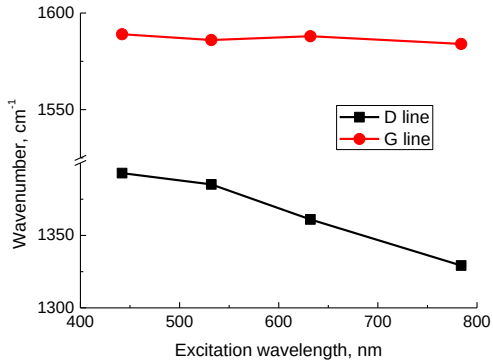

Fig. 5 Dependence of the G and D bands peak positions on the excitation wavelength. The sample was treated with 4.25 J/cm^2 irradiation dose.

3.2. Electrochemical analysis

Fig. 6 presents characteristics of the cyclic voltammetry of the bare and modified ITO recorded in 0.1 M KCl solution. A reduction wave was recorded at -0.8 V at the bare ITO electrode during the scan going towards negative potentials. This reduction also occurred at negative potentials in the backward scan, but it was shifted towards less negative potentials. As seen from the red curve in Fig. 6, the electrode modification with the G2 film induced a shift of the position of the reduction wave to the less negative potential values.

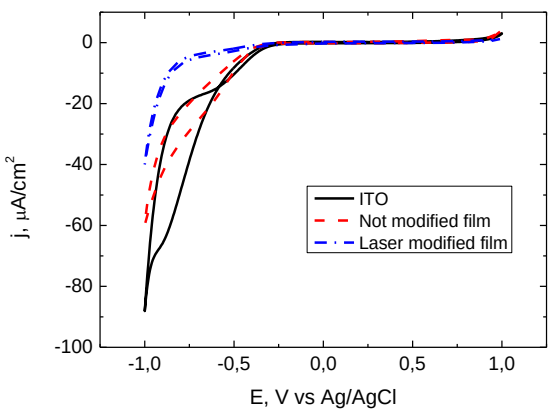

Fig. 6 CVs at ITO, G2 and laser irradiated G2 in 0.1 mol/l KCl. The potential scan rate was 100 mV/s, irradiation dose 1 J/cm^2.

The Electrochemical Impedance Spectroscopy spectra were recorded at the differently modified electrodes: bare ITO, G1-G4, and the same electrodes irradiated with the picosecond laser using various potentials over the whole potential range used in the CV investigation: -0.75; -0.50; 0.00; 0.50; 0.75; 1.00 V. Graphene concentration was varied from 0 to 3 mg/ml.

Fig. 7 presents the complex-plane impedance spectra at various potentials measured with differently modified electrodes before and after laser irradiation. The charge separation was dominating in the double

layer region at 0 V as the complex-plane EIS spectra have a linear shape (Fig. 7a), and all spectra of differently modified electrodes were similar. In all cases, the impedance values rose after the laser irradiation, especially clearly visible at low graphene concentrations.

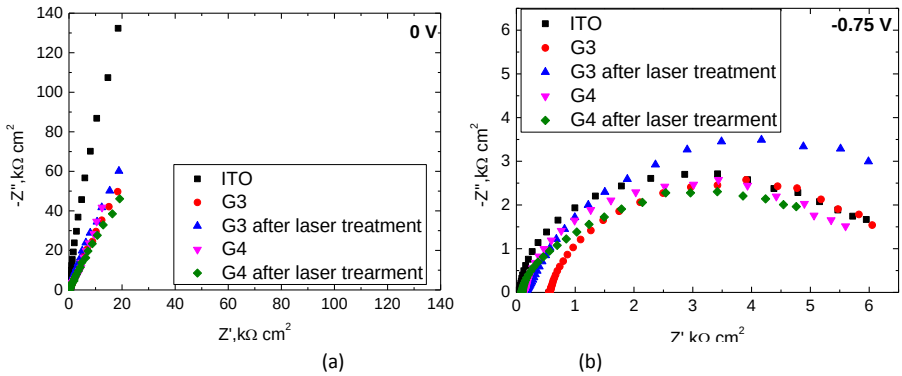

Fig. 7 Complex plane EIS spectra at ITO, untreated and laser-treated graphene-chitosan films measured at 0 v (a) and -0.75 V (b) potentials in 0.1 M KCl. Laser irradiation dose 1 J/cm^2.

From the EIS data, the double layer region capacitance C_{dl} was evaluated applying equivalent electric diagrams. The capacitance C_{dl} increased after the laser treatment. Linear rice of the capacitance occurred when the laser irradiation dose was increased (Fig. 8). This fact suggests that the laser treatment improved electrochemical properties of the G-Chit modified electrode due to creation the edge defects and formation of nanocrystalline structures from graphene flakes after the laser treatment . (Celiešiūtė et al. 2014)

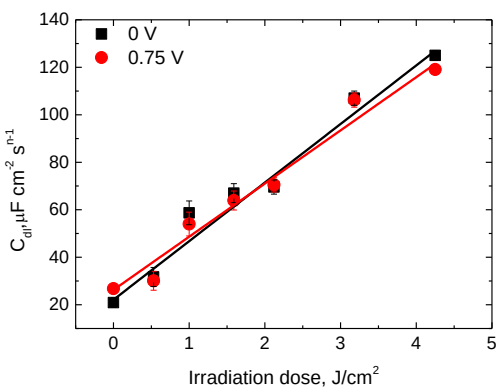

Fig. 8 Dependence of the capacitance calculated from EIS data at 0 V and 0.75 V on the laser irradiation dose in G3 sample.

3.3. Uniform modification of graphene –chitosan film

Uniform modification of the graphene-chitosan film was implemented by picking such values of the beam scanning speed and hatch; that pulse overlap would be homogeneous in the scanning direction and in the perpendicular direction. For such overlapping type, the pitch parameter was introduced. It describes the distance between sequent pulses. The above-described configuration of laser parameters allows minimization of process variables as a variation of the pitch includes variation in scanning speed and hatch

simultaneously. Therefore, only laser power and pitch were changed during these experiments. Experiments were performed with 1064 nm and 532 nm irradiation of the picosecond laser at the constant pulse repetition rate of 100 kHz.

No significant changes in film morphology were observed at irradiation powers beneath 50 mW for both laser wavelengths. At laser power of 300 mW and higher, ablation of the film took place. Significant changes in the Raman spectra were observed at the 100 mW irradiation power using the 1064 nm wavelength (Fig. 10). When higher laser power was applied, the Raman spectra corresponded to amorphous carbon spectra.

The increase of the D- and G-bandwidth was observed after the laser treatment. Such conditions correspond to increasing disorder. Meanwhile, 2D-band intensity decreased. The I_D/I_G and I_{2D}/I_G ratios were evaluated to clarify the amount of defects in the graphene-chitosan after the laser treatment (Fig. 9). The intensity of the 2D-band, corresponding to graphene phase was gradually rising as the pulse overlap decreased (pitch parameter increased). The opposite behaviour was observed for the D-band intensity meaning the decrease in the number of defects in the irradiated film. Thus, the amount of the defects can be controlled in a fine manner with the picosecond laser irradiation using the 100 mW mean power at the 1064 nm wavelength.

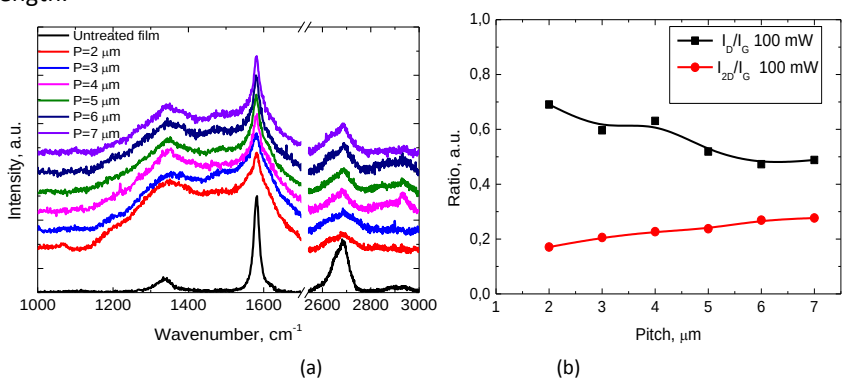

Fig. 9 Raman spectra dependence on the pitch parameter applying the 100 mW 1064 nm picosecond laser irradiation (a), dependence of ID/IG and I2D/IG ratios on the pitch parameter (b).

Results differed in the case of the 532 nm irradiation (Fig. 10). Similar to the 1064 nm irradiation, the broadening of the D- and G-bands was observed at the high pulse overlap conditions using the 100 mW average power. The change of the D- and 2D-band intensities was not as regular as with the 1064 nm irradiation (Fig. 10 b). The I_{2D}/I_G ratio decreased at the pitch of 3 μm, but then it increased more rapidly than after the 1064 nm treatment. The value of I_{2D}/I_G ratio was twice higher at the 6 μm and 7 μm pitch compared to 1064 nm. On the other hand, the I_D/I_G ratio dependence was more irregular using the 532 nm irradiation.

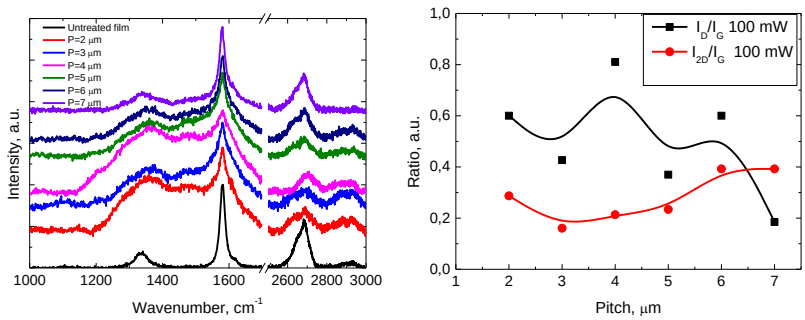

Fig. 10 Raman spectra dependence on the pitch parameter applying the 100 mW, 532 nm picosecond laser irradiation (a), dependence of ID/IG and I2D/IG ratios on the pitch parameter (b).

At the mean laser power lower than 100 mW, no changes in the spectra were observed after the 1064 nm laser treatment while, after the 532 nm treatment, the spectra differed from the untreated graphene-chitosan film. Due to lower modification, the 2D-band intensity was higher than for the 100 mW modification, and fewer defects were present. Dependence of the I_D/I_G and I_{2D}/I_G ratio on the pitch parameter was not as strong as with 100 mW irradiation.

Morphology of the laser treated film area exhibited distinct differences depending on the laser irradiation wavelength. SEM images of 2 μm pitch were chosen to compare surface modifications. At the same irradiation power of 100 mW and 2 μm pitch, forming of the porous structure was observed (Fig. 11). After the 532 nm irradiation treatments, the density of the pores was much higher than that after the 1064 nm treatment.

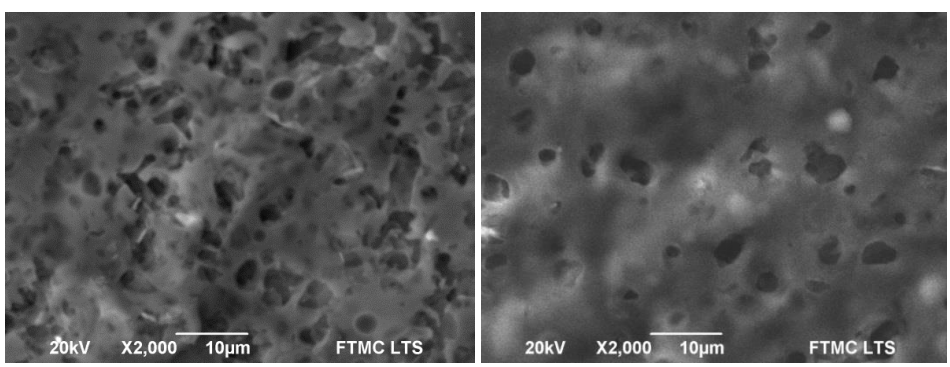

Fig. 11 SEM image of the laser treated graphene-chitosan film. Laser parameters: 100 mW, pitch-2 μm: a) 532 nm; b) 1064 nm.

The size and density of pores determine the structural defects of the graphene-chitosan film. On the other hand, porous structure indicates an increase of the surface area, which is a very helpful feature for sensing applications.

4. Conclusions

The Raman spectroscopy showed that laser irradiation can cut out graphene sheets in the graphene-chitosan composites into smaller pieces inducing more edge defects and the higher graphene load – the larger amount of side defects appeared after the laser treatment. The high laser irradiation dose resulted in the nanocrystalline graphene formation and a significant reduction in the thickness of the graphene-chitosan film.

Picosecond laser irradiation caused an increase in capacitance at the electrode surface due to the formation of graphene nanocrystals. Electrochemical investigation of the laser treated G-Chit/ITO samples proved that such composite electrodes are promising material to be used as a substrate for sensor development.

Uniform modification of graphene-chitosan composites allowed gradual controlling of defects in the material.

Acknowledgements

This research was funded by the European Social Fund under the Global Grant measure, Project No. VP1-3.1-ŠMM-07-K-01-124.

References

Choi W., Lahiri, I., Seelaboyina, R., Kang, Y. S., 2010. Synthesis of Graphene and Its Applications: A Review, Critical Reviews in Solid State and Materials Sciences 35(1), p.52.

Ferrari A. C., Robertson, J., 2000. Interpretation of Raman spectra of disordered and amorphous carbon, Physical Review 61(20), p.14095.

Wang Z., Huang, X., Xue, R., Chen, L., 1998. Dispersion effects of Raman lines in carbons, Journal of Applied Physics84(1), p.227.

Celiešiūtė R., Trusovas, R., Niaura, G., Švedas, V., Račiukaitis, G., Ruželė, Ž.. Pauliukaite R., 2014. Influence of the laser irradiation on the electrochemical and spectroscopic peculiarities of graphene-chitosan composite film,. Electrochimica Acta, 132, p.265.

Trusovas R., Ratautas, K., Račiukaitis, G., Barkauskas, J., Stankevičienė, I., Niaura, G., Mažeikienė R.., 2013. Reduction of graphite oxide to graphene with laser irradiation, Carbon 52, p.574.

Chang H.-W., Tsai, Y.-C., Cheng, C.-W., Lin, C.-Y., Wu, P.-H., 2012. Reduction of graphene oxide in aqueous solution by femtosecond laser and its effect on electroanalysis, Electrochemistry Communications 23, p 37.

Trusovas R., Račiukaitis, G., Barkauskas, J., Mažeikienė, R., 2012. Laser Induced Graphite Oxide/Graphene Transformation. Journal of Laser Micro/Nanoengineering,7(1), p. 49.

Sokolov D. A., Shepperd, K. R., Orlando, T. M., 2010. Formation of Graphene Features from Direct Laser-Induced Reduction of Graphite Oxide. The Journal of Physical Chemistry Letters,1(18), p.2633.